

Thallium  $\pi$ -Cation Complexation by Calix[4]tubes:  $^{205}\text{Tl}$  NMR and X-ray EvidenceSusan E. Matthews,<sup>†,‡</sup> Nicholas H. Rees,<sup>†</sup> Vitor Felix,<sup>§,||</sup> Michael G. B. Drew,<sup>§</sup> and Paul D. Beer<sup>\*†</sup>*Inorganic Chemistry Laboratory, Department of Chemistry, University of Oxford, South Parks Road, Oxford OX1 3QR, U.K., and Department of Chemistry, University of Reading, Whiteknights, Reading RG6 6AD, U.K.*

Received July 18, 2002

Thallium cation complexation by calix[4]tubes has been investigated by a combination of  $^{205}\text{Tl}$ ,  $^1\text{H}$  NMR and ES MS demonstrating the solution formation of a dithallium complex in which the cations are held in the calix[4]arene cavities. In addition, the structure of the complex has been determined in the solid state revealing the cations to be held exclusively by  $\pi$ -cation interactions. Furthermore, this crystal structure has been used as the basis for molecular dynamics simulations to confirm that binding of the smaller  $\text{K}^+$  cation in the calix[4]tube cryptand like array occurs via the axial route featuring a  $\pi$ -cation intermediate.

## Introduction

Thallium has long been proposed as a suitable probe for alkali metal cations in biological systems due to its chemical similarity to group 1 metals and favorable size comparison with potassium ( $\text{Tl}^+$ , 1.44 Å;  $\text{K}^+$ , 1.33 Å).<sup>1</sup> However, a particular advantage of thallium over potassium is its NMR properties, having a spin  $I = 1/2$  nucleus with high natural abundance, good NMR sensitivity, and a large chemical shift range,<sup>2</sup> which allow facile analysis of binding behavior and determination of cation selectivity.

In the late 1970s, thallium NMR was developed as a method for determining the relative stability of complexes of alkali metal cations with a range of crown ethers and to probe the solvent independence of complexation in thallium cryptates.<sup>3</sup> More recently, thallium NMR has been elegantly

applied to the metallocryptands developed by Catalano et al. to demonstrate complexation solely through auro- and metallophilic interactions.<sup>4</sup> However, little interest has been shown in the complexation of thallium by calix[4]arene derivatives<sup>5</sup> and the potential role of  $\pi$ -cation interactions<sup>6</sup> in enabling binding within the macrocyclic cavity.

Recently, we described a new class of ionophore, the calix[4]tube, based on a bis(calix[4]arene) scaffold, which shows exceptional selectivity for complexation of potassium over all other group 1 metals (Figure 1).<sup>7</sup> The similarity between the coordination properties of potassium and thallium in combination with the slight size discrepancy prompted us to investigate the thallium complexation behavior of calix[4]tubes to elucidate further the binding requirements and the route of potassium cation entry. Combining both  $^1\text{H}$  and  $^{205}\text{Tl}$  NMR techniques uniquely enables investigation of the real-time complexation process from the perspectives of both the host and guest species. In addition single-crystal X-ray

\* To whom correspondence should be addressed. E-mail: paul.beer@chem.ox.ac.uk. Tel: +44 1865 272600. Fax: +44 1865 272690.

<sup>†</sup> University of Oxford.

<sup>‡</sup> Current address: Department of Chemistry, Trinity College, University of Dublin, Dublin 2, Ireland.

<sup>§</sup> University of Reading.

<sup>||</sup> On sabbatical leave from the Departamento de Quimica, Universidade de Aveiro, P-3810-193, Aveiro, Portugal.

- (1) Douglas, K. T.; Bunni, M. A.; Baindur, S. R. *Int. J. Biochem.* **1990**, *22*, 429. Manners, J. P.; Morallee, K. G.; Williams, R. J. P. *J. Chem. Soc. D* **1970**, 965.
- (2) Hinton, J. F.; Metz, K. R.; Briggs, R. W. *Prog. Nucl. Magn. Reson. Spectrosc.* **1988**, *20*, 423.
- (3) (a) Srivanavit, C.; Zink, J. I.; Dechter, J. J. *J. Am. Chem. Soc.* **1977**, *99*, 5876. (b) Shamsipur, M.; Popov, A. I. *Inorg. Chim. Acta* **1980**, *43*, 243. (c) Shamsipur, M.; Rounaghi, G.; Popov, A. I. *J. Solution Chem.* **1980**, *9*, 701. (d) Gudlin, D.; Schneider, H. *Inorg. Chim. Acta* **1979**, *33*, 205.

- (4) Catalano, V. J.; Bennet, B. L.; Kar, H. M.; Noll, B. C. *J. Am. Chem. Soc.* **1999**, *121*, 10235. Catalano, V. J.; Bennet, B. L.; Yson, R. L.; Noll, B. C. *J. Am. Chem. Soc.* **2000**, *122*, 10056.
- (5) Couton, D.; Mocerino, M.; Rapley, C.; Kitamura, C.; Yoneda, A.; Ouchi, M. *Aust. J. Chem.* **1999**, *52*, 227. Kimura, K.; Tatsumi, K.; Yokoyama, M.; Ouchi, M.; Mocerino, M. *Anal. Commun.* **1999**, 36, 229.
- (6) Gokel, G. W.; Barbour, L. J.; De Wall, S. L.; Meadows, E. S. *Coord. Chem. Rev.* **2001**, *222*, 127–154. Meadows, E. S.; De Wall, S. L.; Barbour, L. J.; Gokel, G. W. *J. Am. Chem. Soc.* **2001**, *123*, 3092–3107.
- (7) (a) Schmitt, P.; Beer, P. D.; Drew, M. G. B.; Sheen, P. D. *Angew. Chem., Int. Ed. Engl.* **1997**, *36*, 1840. (b) Matthews, S. E.; Schmitt, P.; Felix, V.; Drew, M. G. B.; Beer, P. D. *J. Am. Chem. Soc.* **2002**, *124*, 1341–1353.

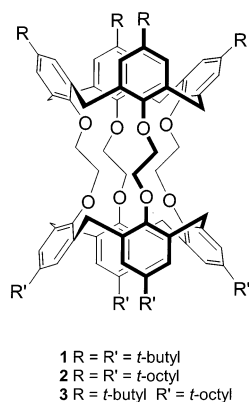


**Figure 1.** Calix[4]tubes.

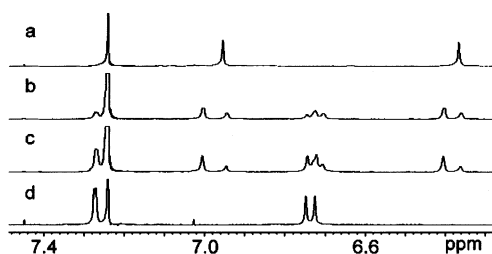


**Figure 2.** Expansion of the aromatic region of the  $^1\text{H}$  NMR spectra for calix[4]tube **2**: (a) uncomplexed; (b) after 60 min; (c) after 120 min; (d) after 12 h (20 equiv of  $\text{TlPF}_6$ ,  $\text{CDCl}_3/\text{CD}_3\text{OD}$  (4:1), 291 K).

analysis reveals thallium cation complexation occurs through calix[4]arene  $\pi$ -cation interactions producing a unique bis-(thallium) calix[4]tube structure.

### NMR Thallium Binding Investigations

We have previously shown from  $^1\text{H}$ NMR kinetic studies that the rate of complexation of potassium and silver cations in the cryptand like cavity of the calix[4]tube is dependent upon both the nature of the upper rim substituent and the counteranions present.<sup>7–9</sup> Taking the latter factor into account, thallium hexafluorophosphate was the salt of choice in all complexation studies.

Initially,  $^1\text{H}$  NMR observations were undertaken on calix[4]tubes (**1–3**) using our standard procedure: solid–liquid extraction of a 20-fold excess of  $\text{TlPF}_6$  in  $\text{CDCl}_3/\text{CD}_3\text{OD}$  (4:1), the solvent mixture being dictated by the low solubility of the ligands in the majority of solvents.<sup>7</sup> Slow complexation of the cation on the NMR time scale resulted in the appearance of new peaks in the aromatic region, with little perturbation of the polyether region, indicating that structural rearrangement of the calix[4]tubes occurred to accommodate the guest metal (Figure 2).

The spectra for all ligands simplified over time to indicate only one species present, a calix[4]tube of considerably lower symmetry than the effective  $C_{2v}$  of the parent ligands. Four (calix[4]tube **1** and **2**) or eight (calix[4]tube **3**) aromatic

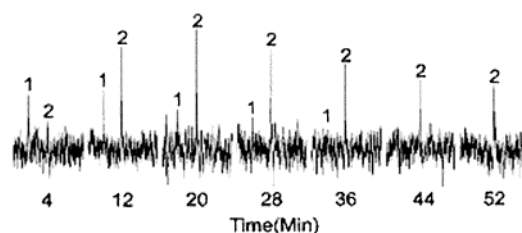


**Figure 3.** Combined  $^{205}\text{Tl}$  spectra for calix[4]tube **1** with spectra recorded at 8 min intervals (20 equiv of  $\text{TlPF}_6$ ,  $\text{CDCl}_3/\text{CD}_3\text{OD}$  (4:1), 298 K). Key: 1,  $1(\text{Tl})$ ; 2,  $1(\text{Tl}_2)$ .

**Table 1.**  $^{205}\text{Tl}$  NMR Shifts (ppm) for  $\text{Tl}$ –Calix[4]tube Complexes

calix[4]tube	monocomplex <i>tert</i> -butyl	dicomplex <i>tert</i> -butyl	monocomplex <i>tert</i> -octyl	dicomplex <i>tert</i> -octyl
<b>1</b>	–580	–627		
<b>2</b>			–560	–607
<b>3</b>	not obsd	–635	–555	–600

resonances were observed which suggests inequivalence of all aromatic residues and that the calix[4]arene units adopt an approximate flattened cone arrangement. The magnitude of the  $^1\text{H}$  NMR shifts which are particularly large in the aromatic region (between 0.35 and 0.4 ppm) combined with the reduction in symmetry suggested that the binding of thallium occurs at the calix[4]arene upper rim through a regional  $\pi$ -cation interaction.

The complex  $^1\text{H}$  NMR changes on binding precluded measurement of relative rates of complexation for the different members of the calix[4]tube family. However  $^{205}\text{Tl}$  NMR, in which small changes in environment greatly affect the thallium resonance, enables clear and direct observation of the complexation process.

Uptake of thallium was monitored for a 2 h period at 8 min intervals, with the temperature held at 298 K, to allow direct comparison between the three calix[4]tubes. The symmetrical calix[4]tubes **1** and **2** showed similar spectra (Figure 3 for **1**). Complexation was slow with formation and gradual decline of an intermediate species, not identifiable in the  $^1\text{H}$  NMR spectra, and development of a final complex which was stable for a period of days. The observed shifts ( $\delta$  –599 to –634 ppm, Table 1) are not consistent with binding within the cryptand-like oxygen array. Previous studies with the structurally similar 2.2.2-cryptand have shown that when the coordination sphere of the cation is fully satisfied by donor groups, the thallium shift occurs at approximately  $\delta$  62 ppm and is unaffected by solvent.<sup>3d</sup>

It can be proposed that the two signals observed when employing this excess of cation relate first to binding of one cation (the intermediate) and later to binding of two cations (the final complex) through  $\pi$ -cation interactions at the calix[4]arene upper rims. The ability to observe the intermediate species offers a particular advantage to the use of thallium NMR techniques.

The binding process can be further elucidated when the asymmetric calix[4]tube **3** is considered (Figure 4). Here, the final complex gives two thallium resonances which can be directly related by their shifts to binding of a thallium cation in each of the two different calix[4]arene units (Table 1). Of particular interest, in this case, is the observation of

(8) Matthews, S. E.; Felix, V.; Drew, M. G. B.; Beer, P. D. *Chem. Phys. Phys. Chem.* **2002**, *4*, 3849–3858.

(9) Evidence of binding within the cryptand cavity<sup>7</sup> with  $\text{AgPF}_6$  is in direct contrast to the studies of Budka et al. using  $\text{AgTl}$  adding further evidence on the importance of counterions in complexation: Budka, J.; Lhotak, P.; Stibor, I.; Michlova, V.; Sykora, J.; Cisarova, I. *Tetrahedron Lett.* **2002**, *43*, 2857–2861.

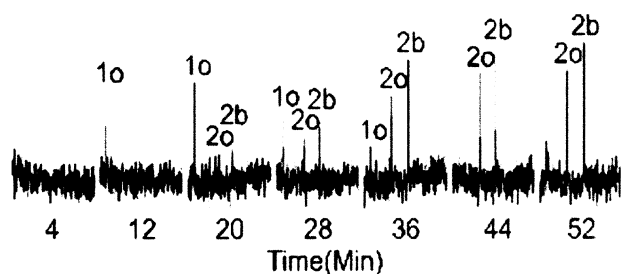


**Figure 4.** Combined  $^{205}\text{Tl}$  spectra for calix[4]tube **3** with spectra recorded at 8 min intervals (20 equiv of  $\text{TlPF}_6$ ,  $\text{CDCl}_3/\text{CD}_3\text{OD}$  (4:1), 298 K). Key: 1o,  $3(\text{Tl})$  (monocomplex signal for binding in *tert*-octylcalix[4]arene); 2o,  $3(\text{Tl}_2)$  (dicomplex signal for binding in *tert*-octyl region); 2b,  $3(\text{Tl}_2)$  (dicomplex signal for binding in *tert*-butyl region).

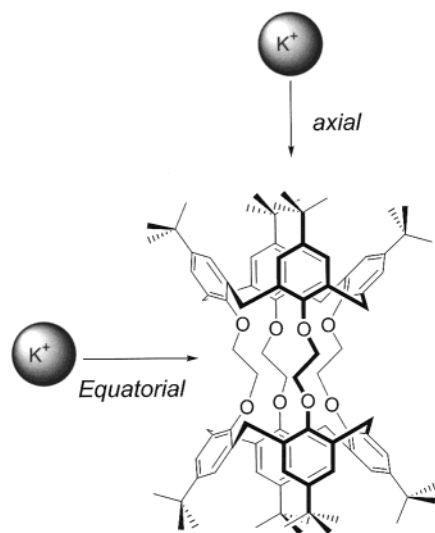


**Figure 5.** Comparison of axial and equatorial routes of potassium entry into calix[4]tubes.

only one thallium resonance for the monocation species. Given the range in NMR shifts observed for the binding of thallium within different calix[4]arene subunits, it is possible to assign this peak, by spectral comparison, to binding at the *tert*-octyl region and it is unlikely to be a coincident signal of both monocation species. While the reason for this observation is unknown, it can be postulated that either preferential binding of the first cation in the *tert*-octylcalix[4]arene occurs or there is rapid conversion of the *tert*-butyl monocation to the dication, rendering the signal too transient for measurement.

Formation of the dication is fastest for calix[4]tube **1** (25% intermediate complex formed after 5 min), with calix[4]tubes **2** and **3** showing slower uptake. This is in direct accordance with the results obtained for potassium binding, giving further credence to the binding model for potassium,<sup>7,8</sup> entry through the axial route with a multistep binding process including initial  $\pi$ -cation interactions (Figure 5).

### X-ray Structure

The proposed multication binding by the calix[4]tubes has been confirmed by the solid-state structure of the thallium complex of calix[4]tube **2**. Single crystals of X-ray quality were prepared by slow diffusion of methanol into a solution of the complex in 4:1 chloroform/methanol.<sup>10</sup> The structure

consists of discrete  $2(\text{Tl}_2^{2+})$  cations and  $\text{PF}_6^-$  anions. The cation has crystallographic  $2/m$  symmetry, and one ordered cation is shown in Figure 6. The conformation of the cage can be quantified by the  $\text{O}-\text{CH}_2-\text{CH}_2-\text{O}$  torsion angles ( $154.1$ ,  $22.9$ ,  $-154.1$ ,  $-22.9^\circ$ ) and the angles made by the phenyl rings with the plane of the methylene groups ( $82.7 \times 2$ ,  $36.7$ ,  $45.1^\circ$ ). The conformation of the linkage can therefore be described as  $t\bar{g}t\bar{g}$  ( $t = \text{trans}$ ,  $g = \text{gauche}$ ). The *gauche* linkages are bonded to two phenyl rings that are nearly vertical, parallel to the cage axis, while the *trans* linkages lead to the semihorizontal phenyl rings.

This can be compared to the values for the uncomplexed host **2** (Figure 7),<sup>7b</sup> in which the torsion angles are similar but the four phenyl rings intersect the plane of the 4 methylene atoms at angles of  $83.3$ ,  $37.4$ ,  $88.9$ , and  $31.2^\circ$ , thus indicating that a less flattened structure is adopted on complexation of the metal.

The molecule contains two  $\text{Tl}^+$  cations in equivalent positions, and close contacts from the  $\text{Tl}^+$  to atoms in the calix[4]tube are listed in Table 2. The cation is bonded to all 12 carbon atoms of the two vertical phenyl rings ( $\text{Tl}-\text{C}$   $3.15(1)$ – $3.37(1)$  Å) and also to the two oxygen atoms bonded to the semihorizontal phenyl rings ( $2.933(10)$ ,  $3.064(10)$  Å). There are also close contacts with the bottom carbon of these rings ( $3.139(14)$ ,  $3.176(14)$  Å), but all other  $\text{Tl}-\text{C}$  distances to these rings are greater than  $3.5$  Å. Although there are over 40 examples in the Cambridge Crystallographic Database of  $\text{Tl}$  bonded to aromatic rings, most involve negatively charged cyclopentadienyl groups where  $\text{Tl}-\text{C}$  distances are usually in the range of  $2.80$ – $3.00$  Å. However, there are a few examples of  $\text{Tl}^+$  bonded to neutral phenyl rings, including bis( $\eta^6$ -mesitylene)thallium, tetratrate boron,<sup>11</sup> and a bis( $\eta^6$ -toluene)thallium complex,<sup>12</sup> where  $\text{Tl}-\text{C}$  distances range from  $3.12$  to  $3.22$  and  $3.21$  to  $3.35$  Å, respectively. Equally although a number of structures of calix[4]arene  $\pi$ -cation complexes have been reported with cesium,<sup>13</sup> potassium,<sup>14</sup> and silver cations,<sup>15</sup> this is the first example involving thallium and showing two cations in such close contact by virtue of the unique bis(calix[4]arene) structure.

- (10) Crystallographic data (excluding crystallographic structural factors) for the structures reported in this paper have been deposited with the Cambridge Crystallographic Data Centre as supplementary publication no. CCDC-166950. Copies of the data can be obtained free of charge on application to The Director, CCDC, 12 Union Road, Cambridge CB2 1EZ, U.K. (Fax: int. code +1223 336-033. E-mail: deposit@chemcryst.cam.ac.uk.)
- (11) Noirod, M. D.; Anderson, O. P.; Strauss, S. H. *Inorg. Chem.* **1987**, *26*, 2216.
- (12) Mathur, R. S.; Drovetskaya, T.; Reed, C. A. *Acta Crystallogr., Sect. C* **1997**, *53*, 881.
- (13) Leverd, P. C.; Berthault, P.; Lance, M.; Nierlich, M. *Eur. J. Inorg. Chem.* **1998**, 1859–1862. Harrowfield, J. M.; Ogden, M. I.; Richmond, W. R.; White, A. H. *J. Chem. Soc., Chem. Commun.* **1991**, 1159–1161. Assmus, R.; Böhmer, V.; Harrowfield, J. M.; Ogden, M. I.; Richmond, W. R.; Skelton, B. W.; White, A. H. *J. Chem. Soc., Dalton Trans.* **1993**, 2427–2433.
- (14) Gibson, V. C.; Redshaw, C.; Clegg, W.; Elsegood, M. R. *J. Chem. Commun.* **1997**, 1605–1606. Beer, P. D.; Drew, M. G. B.; Gale, P. A.; Leeson, P. B.; Ogden, M. I. *J. Chem. Soc., Dalton Trans.* **1994**, 3479–3485.
- (15) Xu, W.; Puddephatt, R. J.; Muir, K. W.; Torabi, A. A. *Organometallics* **1994**, *13*, 3054–3062.

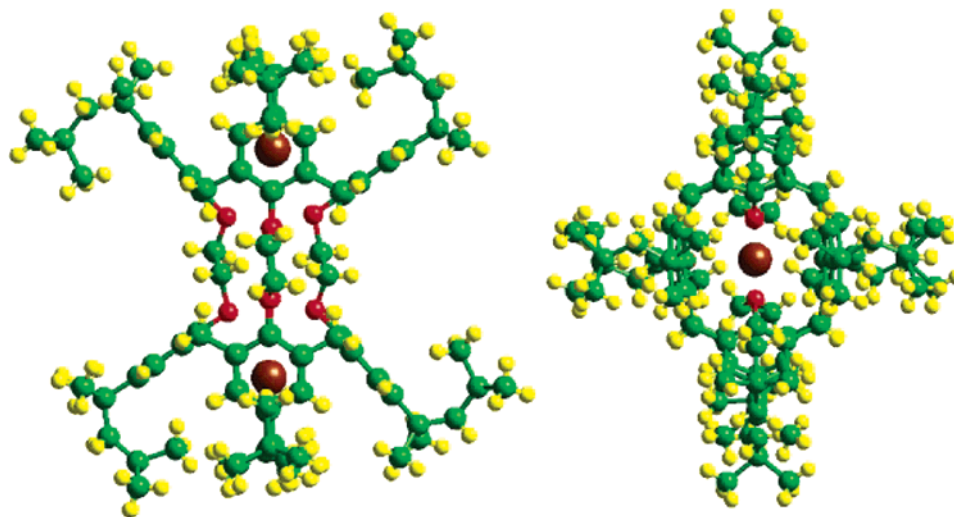


**Figure 6.** Two views of the structure of an ordered molecule of  $2(\text{Tl}_2^{2+})$  (thallium, brown; oxygen, red; carbon, green; hydrogen, yellow): (a) view perpendicular to the main axis of the calix[4]tube; (b) view down the main axis of the calix[4]tube.

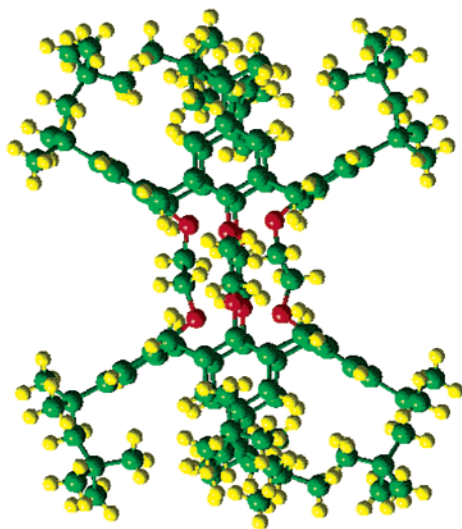


**Figure 7.** Structure of an ordered molecule of **2** (oxygen, red; carbon, green; hydrogen, yellow).

**Table 2.** Dimensions (Å) Involving the  $\text{Tl}^+$  Ions in the Structure of  $2(\text{Tl}_2^{2+})$

Tl–C(11)	3.149(11)	Tl–C(16)	3.207(11)
Tl–C(12)	3.255(11)	Tl–O(250)	2.932(10)
Tl–C(13)	3.366(10)	Tl–O(450)	3.063(10)
Tl–C(14)	3.239(11)	Tl–C(46)	3.139(14)
Tl–C(15)	3.174(10)	Tl–C(26)	3.176(14)

### Mechanism of Insertion of Metals into the Calix[4]-tube

The positions of the thallium atoms in this structure complete the picture for our study of the inclusion of metals in the calix[4]tube and confirm the mechanism suggested in our previous reports.<sup>7,8</sup> The three stages of metal insertion, as characterized by crystal structures, are illustrated in Figure 8a–c. First in Figure 8a the structure of a calix[4]tube host is shown, then as in Figure 8b the metal enters the top of one calix[4]arene and forms an intermediate complex interacting with the aromatic rings, and then as in Figure 8c the metal proceeds into the center of the complex, concomitant with a change in conformation of the calix[4]tube, and

forms bonds to the 8 oxygen atoms. The crystal structures of **1** (Figure 8) and **2** (Figure 7) show the calix[4]tube with the O–CH<sub>2</sub>–CH<sub>2</sub>–O links in the *tg*tg conformation. The crystal structure of  $2(\text{Tl}_2^{2+})$  presented here is characteristic of the intermediate position for any metal entering the calix[4]tube where it is in contact with the aromatic rings, but the conformation of the calix[4]tube at this stage remains unchanged. The third stage in the encapsulation of a metal is characterized by the structure of **1**(K<sup>+</sup>), which contains an approximate though noncrystallographic *C*<sub>4</sub> element of symmetry along the main axis of the molecule. All ethylene linkages present a *gauche* conformation with the O–C–C–O torsion angles taking up values of 68.2, 59.8, 52.3, and 61.9°, so that the conformation of the structure can be described as *gggg*. The angles of intersection of the phenyl rings with the mean plane of the four methylene carbon atoms are similar varying only between 64.6(2) and 67.9(2)°. The potassium ion is located at the center of a slightly flattened cube of the eight oxygen atoms with the K–O distances ranging from 2.759(6) to 2.809(6) Å.

### Modeling Studies

These crystal structures represent static snapshots of the metal insertion reactions. We have also carried out molecular dynamics calculations<sup>7b,8</sup> with K<sup>+</sup>, Tl<sup>+</sup>, and other metals to confirm this reaction path. In these simulations we find that the cation enters the cage along the central axis of the calix[4]tube and is then located at an intermediate position close to the phenyl rings before proceeding to the center of the cage triggering the necessary conformational change of the central O–CH<sub>2</sub>–CH<sub>2</sub>–O torsion angles from *tg*tg to *gggg*, where the oxygen atoms can accommodate the cation in an approximate cubic 8-coordinate environment. However, the size of the cation affects the ease of proceeding from stage b of Figure 8, the intermediate position, to stage c of Figure 8, the central position. Molecular dynamics simulations for K<sup>+</sup> show that the metal can proceed to the center at 400 K within 150 ps of the beginning of the simulation, but in contrast under the same theoretical conditions, the Tl<sup>+</sup> cation

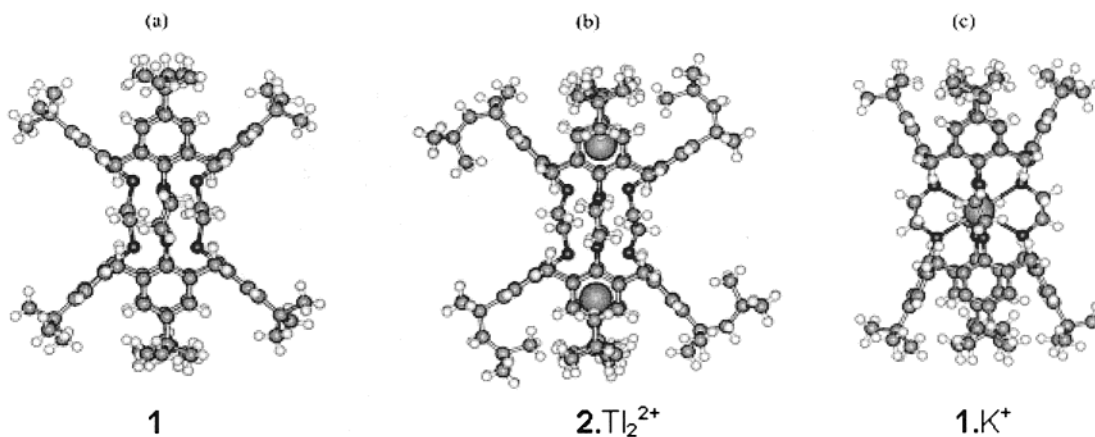


**Figure 8.** Crystal structures of (a) **1**, (b) **2(Tl<sub>2</sub><sup>2+</sup>)**, and (c) **1(K<sup>+</sup>)** illustrating the mechanism for the entry of metal ions into the calix[4]cage.

remains in the position found in the crystal structure of **2(Tl<sub>2</sub><sup>2+</sup>)** reported here and does not enter the cavity unless the temperature is raised significantly to 600 K. For larger cations such as Cs<sup>+</sup>, the metal ion does not enter the cavity even when the temperature is raised to 1000 K, thus illustrating the fact that the restricted size of the entrance to the central cage prevents the entry of the larger cations. A supporting influence in the case of Tl<sup>+</sup> may be the increased stability of the Tl<sup>+</sup> phenyl interactions compared to other cations. However it is clear from previous calculations that the ideal M–O distance within the cavity is 2.82 Å, whereas a search of the CCDC showed K–O and Tl(I)–O distances in comparable structures averaging to 2.84 and 2.94 Å, respectively, confirming the excellent fit of K<sup>+</sup> but not Tl<sup>+</sup> for the central cavity.

### Competitive Binding Studies

Electrospray mass spectroscopy has recently attracted considerable interest for the evaluation of host–guest complexation and ion selectivity with calixcrown systems.<sup>16</sup> These studies have shown that the ions seen in the gas phase accurately reflect the composition of host–guest complexes. In this study the technique has been used to both verify the solution binding properties and offer further insight into the binding process. Electrospray mass spectrometry after 48 h precomplexation with 20 equiv of TlPF<sub>6</sub> in chloroform/methanol (4:1) confirmed that the dithallium cation complex is the dominant species in solution with the ion being detected only as the doubly charged species in addition to a singly charged species for the monothallium complex. Competition experiments after precomplexation with 20equiv of both KPF<sub>6</sub> and TlPF<sub>6</sub> for 48 h gave no evidence for formation of the potassium complex showing peaks of the same intensities for both the mono- and dithallium complexes as observed on complexation of thallium alone (Figure 9), thus suggesting that thallium complexation is fast and of sufficient strength to preclude displacement by potassium.

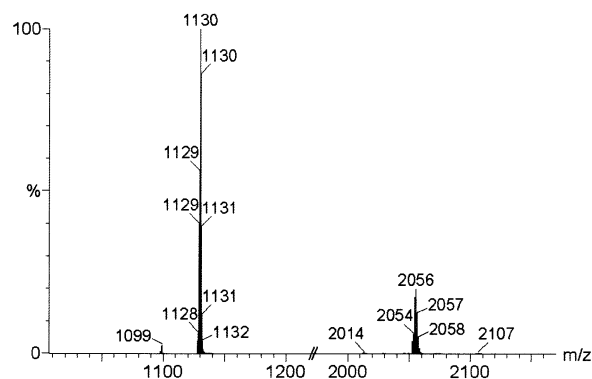


**Figure 9.** ES MS of calix[4]tube **2** after 48 h of complexation with 20 equiv of KPF<sub>6</sub> and TlPF<sub>6</sub> showing the presence of both mono- and dithallium complexes.

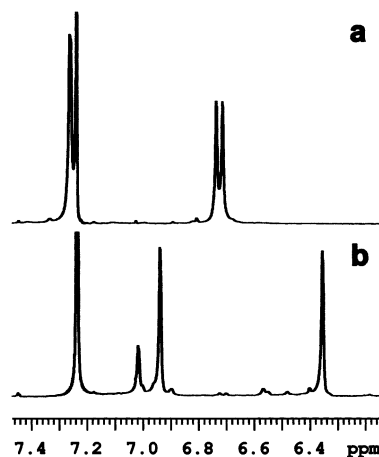


**Figure 10.** Comparison of K<sup>+</sup> uptake by calix[4]tube **2** after 11 h in (a) the presence and (b) the absence of Tl<sup>+</sup>.

Equally, quantitative NMR kinetic experiments showed no potassium complex after 11 h following precomplexation of calix[4]tube **2** with TlPF<sub>6</sub> in contrast to 18% conversion during the same time period under noncompetitive conditions (Figure 10). Indeed comparison of the relative rates of decline of uncomplexed host, in noncompetitive binding studies, confirms that thallium is complexed considerably faster ( $k_{dc}(\text{K}^+) = 0.0028$  s and  $k_{dc}(\text{Tl}^+) = 0.07$  s for calix[4]tube **1**, where  $k_{dc}$  is the rate constant for decline of the uncomplexed host). The conclusion can be drawn that the thallium cations effectively block entry of potassium into the cryptand-like

(16) Allain, F.; Virelizer, H.; Moulin, C.; Jankowski, C. K.; Dozol, J. F.; Tabet, J. C. *Spectroscopy* **2000**, *14*, 127–139. Blanda, M. T.; Farmer, D. B.; Brodbelt, J. S.; Goolsby, B. J. *J. Am. Chem. Soc.* **2000**, *122*, 1486–1491. Goolsby, B. J.; Brodbelt, J. S.; Adou, E.; Blanda, M. T. *Int. J. Mass Spectrom.* **1999**, *193*, 197–204.

cage of the calix[4]tube, providing strong experimental evidence for the previously described molecular modeling studies.

It remains to be considered whether such complexation of thallium, through  $\pi$ -contacts, is a general, although hereto unobserved, property of calix[4]arenes not featuring other potential binding sites. Mocerino and co-workers<sup>5</sup> have reported preliminary data suggesting that allyl derivatized calix[4]arenes can bind thallium although the actual mode of binding was not elucidated. <sup>1</sup>H and <sup>205</sup>Tl NMR studies, under conditions identical with those employed with the calix[4]tubes, with a simple calix[4]arene tetraether reveal no evidence for formation of a  $\pi$ -cation complex. Equally, comparison with the newly reported thiacalix[4]tube,<sup>17</sup> which shows no binding of potassium as a consequence of its enhanced flexibility over calix[4]tubes, failed to show thallium binding. Thus, it may be postulated that the unique fixed flattened cone conformation<sup>7b</sup> of calix[4]tubes is a prerequisite for upper-rim complexation of thallium, although further studies on calix[4]arenes bearing an additional ether binding region may elucidate this further.

## Conclusion

Thallium is found to be exclusively bound in both of the upper-rim cavities of a calix[4]tube through  $\pi$ -cation interactions. Through the use of <sup>205</sup>Tl NMR, in combination with <sup>1</sup>H NMR and electrospray mass spectrometry, this complexation event has been determined to be both rapid and stepwise and the interaction to be of sufficient strength to preclude subsequent binding of potassium. Single-crystal X-ray analysis has confirmed that binding of thallium occurs in the calix[4]arene cavities and provides, in combination with molecular modeling studies, interesting additional evidence for the axial route of potassium entry to calix[4]tubes.

## Experimental Section

All calix[4]tubes were prepared according to literature procedures.<sup>7</sup>

<sup>1</sup>H NMR spectra were acquired at 499.985 MHz on a Varian Unity+ 500 MHz NMR spectrometer and internally referenced to

(17) Matthews, S. E.; Felix, V.; Drew, M. G. B.; Beer, P. D. *New J. Chem.* **2001**, 25, 1355.

the chloroform resonance at  $\delta$  7.24 ppm. <sup>205</sup>Tl NMR spectra were acquired at 173.124 MHz using a 300 MHz magnet with a Varian 500 MHz broad-band probe connected to Varian Unity+ 500 MHz console. The <sup>205</sup>Tl resonant frequencies were scaled to a **B**<sub>0</sub> field where protons resonate at 100 MHz and are referenced to  $\Xi$  57.633 833 MHz.

Crystal data for **2**(Tl<sub>2</sub>)(PF<sub>6</sub>)<sub>2</sub>: C<sub>128</sub>H<sub>184</sub>F<sub>12</sub>O<sub>8</sub>P<sub>2</sub>Tl<sub>2</sub>; *M* = 2549.44; monoclinic, space group *C2/m*; *a* = 20.027(12), *b* = 22.622(14), *c* = 18.669(11) Å;  $\beta$  = 105.84(1); *V* = 8137 Å<sup>3</sup>; *Z* = 2, *d*<sub>m</sub> = 1.041 Mg m<sup>-3</sup>;  $\mu$  = 2.052 mm<sup>-1</sup>. Intensity data were collected with Mo K $\alpha$  radiation using the MARresearch image plate system. The crystal was positioned at 70 mm from the image plate. A total of 100 frames were measured at 2° intervals with a counting time of 10 min to give 13 451 reflections of which 7332 were independent (*R*(int) = 0.0734). Data analysis was carried out with the XDS program<sup>18</sup> The structure was solved using direct methods with the Shelx86 program.<sup>19</sup> The molecule has crystallographic *2/m* symmetry. The two trans -O-CH<sub>2</sub>-CH<sub>2</sub>-O links between the two calix[4]arenes are disordered with the carbon atoms taking up two possible positions. The *tert*-octyl groups were also disordered around the mirror planes. The two PF<sub>6</sub><sup>-</sup> anions were disordered over two sets of general positions each given 0.25 occupancy. An empirical absorption correction was applied using DIFABS.<sup>20</sup> The non-hydrogen atoms were refined with anisotropic thermal parameters. The hydrogen atoms were included in geometric positions and given thermal parameters equivalent to 1.2 times those of the atom to which they were attached. The structure was refined on *F*<sup>2</sup> using Shelxl.<sup>21</sup> The final *R* values were *R*1 = 0.1005 and *wR*2 = 0.2181 for 4822 data with *I* > 2 $\sigma$ (*I*). Details of the structure have been deposited at the CCDC with Reference No. 166950.

**Acknowledgment.** This work was supported by an EPSRC Postdoctoral Fellowship (S.E.M.). The University of Reading and the EPSRC are gratefully acknowledged for funds toward the crystallographic image plate system. V.F. thanks the FCT for a sabbatical leave grant.

**Supporting Information Available:** Crystallographic information files (CIF) for **2**(Tl<sub>2</sub>)(PF<sub>6</sub>)<sub>2</sub>. This material is available free of charge via the Internet at <http://pubs.acs.org>.

IC025884X

(18) Kabsch, W. *J. Appl. Crystallogr.* **1988**, 21, 916–924.

(19) Shelx86: Sheldrick, G. M. *Acta Crystallogr.* **1990**, A46, 467–473.

(20) DIFABS: Walker, N.; Stuart, D. *Acta Crystallogr.* **1983**, A39, 158–166

(21) Sheldrick, G. M. *Shelxl: program for crystal structure refinement*; University of Gottingen: Gottingen, Germany, 1993.